Citation: Molecular Therapy — Methods & Clinical Development (2014) **1,** 14051; doi:10.1038/mtm.2014.51
© 2014 The American Society of Gene & Cell Therapy All rights reserved 2329-0501/14

www.nature.com/mtm

ARTICLE

Widespread gene transfer in the central nervous system of cynomolgus macaques following delivery of AAV9 into the cisterna magna

Christian Hinderer[1], Peter Bell[1], Charles H Vite[2], Jean-Pierre Louboutin[3], Rebecca Grant[1], Erin Bote[1], Hongwei Yu[1], Bryan Pukenas[4], Robert Hurst[4] and James M Wilson[1]

Adeno-associated virus serotype 9 (AAV9) vectors have recently been shown to transduce cells throughout the central nervous system of nonhuman primates when injected into the cerebrospinal fluid (CSF), a finding which could lead to a minimally invasive approach to treat genetic and acquired diseases affecting the entire CNS. We characterized the transduction efficiency of two routes of vector administration into the CSF of cynomolgus macaques—lumbar puncture, which is typically used in clinical practice, and suboccipital puncture, which is more commonly used in veterinary medicine. We found that delivery of vector into the cisterna magna via suboccipital puncture is up to 100-fold more efficient for achieving gene transfer to the brain. In addition, we evaluated the inflammatory response to AAV9-mediated GFP expression in the nonhuman primate CNS. We found that while CSF lymphocyte counts increased following gene transfer, there were no clinical or histological signs of immune toxicity. Together these data indicate that delivery of AAV9 into the cisterna magna is an effective method for achieving gene transfer in the CNS, and suggest that adapting this uncommon injection method for human trials could vastly increase the efficiency of gene delivery.

Molecular Therapy — Methods & Clinical Development (2014) **1**, 14051; doi:10.1038/mtm.2014.51; published online 10 December 2014

INTRODUCTION

Gene therapy using AAV vectors has enormous potential to treat acquired and congenital diseases affecting the central nervous system (CNS). Numerous studies in murine disease models have demonstrated the efficacy of AAV-mediated gene transfer in the brain, and initial human studies have shown an excellent safety profile.[1–5] These pioneering clinical trials were carried out using multiple direct injections of the vector into the brain parenchyma, a strategy which has been shown in preclinical studies to achieve efficient gene transfer to cells surrounding the injection site.[6] However, treatment of diseases affecting cells throughout the CNS will ultimately necessitate a delivery strategy capable of widespread transduction. Simply increasing the number of intraparenchymal injections is not feasible, as even the most promising large animal studies have required at least four injection sites, which would translate to more than 100 injections in an adult human.[6,7] Intravascular (IV) delivery of AAV serotype 9, which can traverse the blood-brain barrier, has been proposed as an alternative approach to achieve widespread transduction in the CNS.[8] While IV delivery is extremely effective in mice, in larger animals transduction in the CNS has been much more restricted.[9,10] This approach is further limited by the extremely large doses required to achieve transduction in the brain and the resulting high off-target transduction of peripheral organs.[8,9]

Several groups have recently reported that delivery of AAV serotypes 7 and 9 into the cerebrospinal fluid (CSF) of nonhuman primates can effect transduction of both neurons and glia throughout the brain and spinal cord.[10–12] This represents a critical advance in the field of CNS gene therapy. It may now be possible not only to achieve gene transfer throughout the CNS in humans, but to do so with a single minimally invasive injection. Access to the subarachnoid CSF is routinely achieved by lumbar puncture in clinical practice for diagnostic purposes and for administration of medications. Although less common, access can also be achieved at the level of the cisterna magna by sub-occipital puncture. Intrathecal AAV delivery therefore represents a relatively low-risk delivery strategy that could be readily translated to the clinic.

In order to advance this approach toward clinical trials, we performed nonhuman primate studies to evaluate the efficiency of two minimally invasive delivery approaches—lumbar puncture and suboccipital puncture—for achieving vector distribution throughout the brain and spinal cord. One previous study reported that both strategies result in transgene expression in the brain, but did not quantitatively compare vector distribution.[12] Based on our findings we estimate that sub-occipital puncture is 10- to 100-fold more efficient for brain transduction, making this approach far more promising for clinical use.

[1]Gene Therapy Program, Department of Pathology and Laboratory Medicine, University of Pennsylvania Perelman School of Medicine, Philadelphia, Pennsylvania, USA; [2]Department of Clinical Studies, School of Veterinary Medicine, University of Pennsylvania, Philadelphia, Pennsylvania, USA; [3]Department of Basic Medical Sciences, Section of Anatomy, University of the West Indies, Kingston, Jamaica; [4]Department of Radiology, Hospital of the University of Pennsylvania, Philadelphia, Pennsylvania, USA.
Correspondence: JM Wilson (wilsonjm@mail.med.upenn.edu)
Received 22 August 2014; accepted 5 September 2014

In addition, we performed detailed evaluation of histological markers of inflammation in the CNS of treated animals. Several studies have found intrathecal delivery of AAV9 to be safe in nonhuman primates and other species, although one group has reported that macaques treated with a vector carrying a GFP transgene experienced neurological deficits associated with histological evidence of an inflammatory response.[13] We found that treated animals exhibited no clinical or histological abnormalities, although CSF lymphocytes were elevated in some animals. Overall, our data suggest that intrathecal AAV injection by suboccipital puncture could serve as a useful gene transfer method for the treatment of neurological disease.

RESULTS

Intracisternal delivery achieves broader vector distribution in the CNS

We treated six cynomolgus macaques with an intrathecal injection of a single-stranded AAV9 vector expressing GFP from either the cytomegalovirus (CMV) or chicken beta-actin (CB) promoter (Table 1). Four of the animals were injected via sub-occipital puncture; two were treated via lumbar puncture. There were no adverse clinical events during the course of the study. All animals were sacrificed 14 days after injection for histological analysis.

Table 1 Summary of study subjects

Animal #	*ROA*	*Vector*	*Dose*	*Weight (kg)*	*Sex*	*Age*
17	CM	AAV9.CMV.eGFP	5×10^{12} GC/kg	3.60	F	8 years
18	CM	AAV9.CB7.eGFP	5×10^{12} GC/kg	3.85	F	8 years
20	CM	AAV9.CB7.eGFP	2.5×10^{12} GC/kg	5.40	F	8 years
21	CM	AAV9.CB7.eGFP	2.5×10^{12} GC/kg	8.75	F	8 years
04	L	AAV9.CB7.eGFP	2.5×10^{12} GC/kg	4.25	F	8 years
05	L	AAV9.CB7.eGFP	2.5×10^{12} GC/kg	4.85	F	8 years
49	IV	AAV9.CMV.eGFP	2.0×10^{13} GC/kg	3.30	F	8 years

CM, cisterna magna; F, female; IV, intravenous; L, lumbar injection; ROA, route of administration.

Vector distribution was evaluated in CNS and peripheral tissues by quantitative PCR (Figure 1). All animals treated by suboccipital puncture exhibited substantial vector deposition in the brain and spinal cord, with up to one vector genome per cell in most regions. Animals treated by lumbar puncture had approximately tenfold lower gene transfer throughout the spinal cord, and up to 100-fold less in the brain. In contrast, both groups had similar distribution to peripheral organs. Vector copy numbers were quite high in liver and spleen, indicating significant vector escape to the peripheral circulation.

As previous studies have demonstrated the ability of AAV9 to transduce cells within the CNS following intravascular injection, we treated one rhesus macaque intravenously to compare the efficiency of this approach to intrathecal injection (Figure 1). Despite the use of a high vector dose (2×10^{13} GC/kg) and the absence of detectable neutralizing antibodies to AAV9 in this animal, vector distribution to the CNS was substantially lower than that achieved at four- to eightfold lower doses via cisternal injection. Due to the low CNS gene transfer efficiency observed in this animal we did not explore this route of administration further.

GFP false positives complicate assessment of transgene expression in the CNS

We initially attempted to quantify GFP expressing cells in the CNS by immunohistochemistry (IHC), as other groups have previously utilized this method to measure GFP expression in the nonhuman primate CNS.[11,12] We identified what appeared to be a large number of GFP positive cells throughout the CNS of treated macaques (Supplementary Figure S1a,c). However, we also detected a similar staining pattern in some negative control brain tissues from animals that had not received a GFP expressing vector (Supplementary Figure S1b,d). The false-positive neurons appeared dark on H&E sections, a property consistent with the "dark neuron" artifact that has

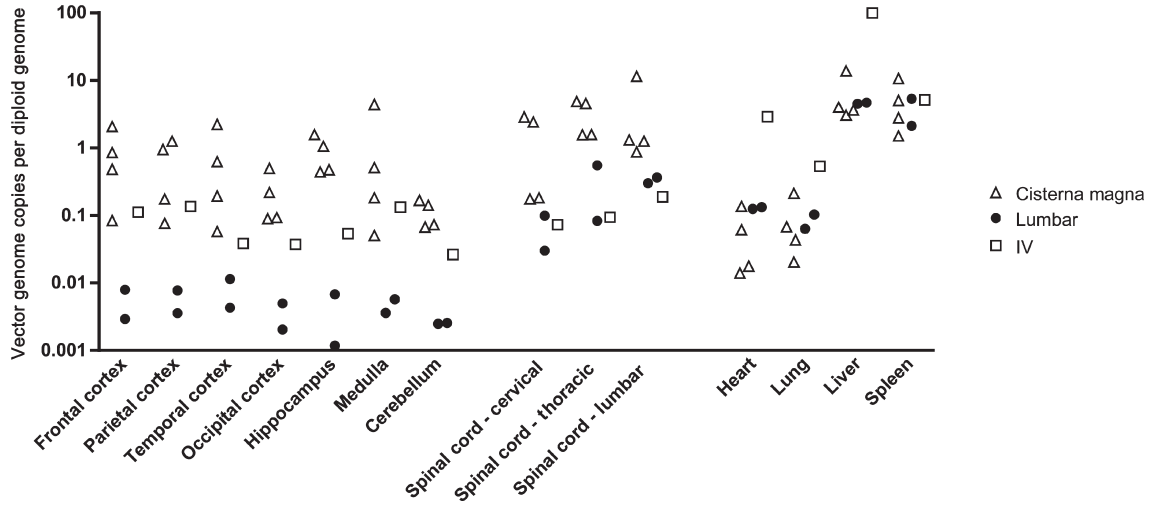

Figure 1 AAV9 biodistribution following intrathecal delivery in nonhuman primates. AAV9 was administered to six cynomolgus macaques at doses of $2.5–5\times10^{12}$ GC/kg by injection into the cisterna magna ($n=4$) or the lumbar subarachnoid space ($n=2$). An additional animal was treated intravenously with a high dose (2×10^{13} GC/kg) of AAV9. All animals were sacrificed 2 weeks after injection and vector genomes were quantified in tissue samples by Taqman PCR.

© 2014 The American Society of Gene & Cell Therapy

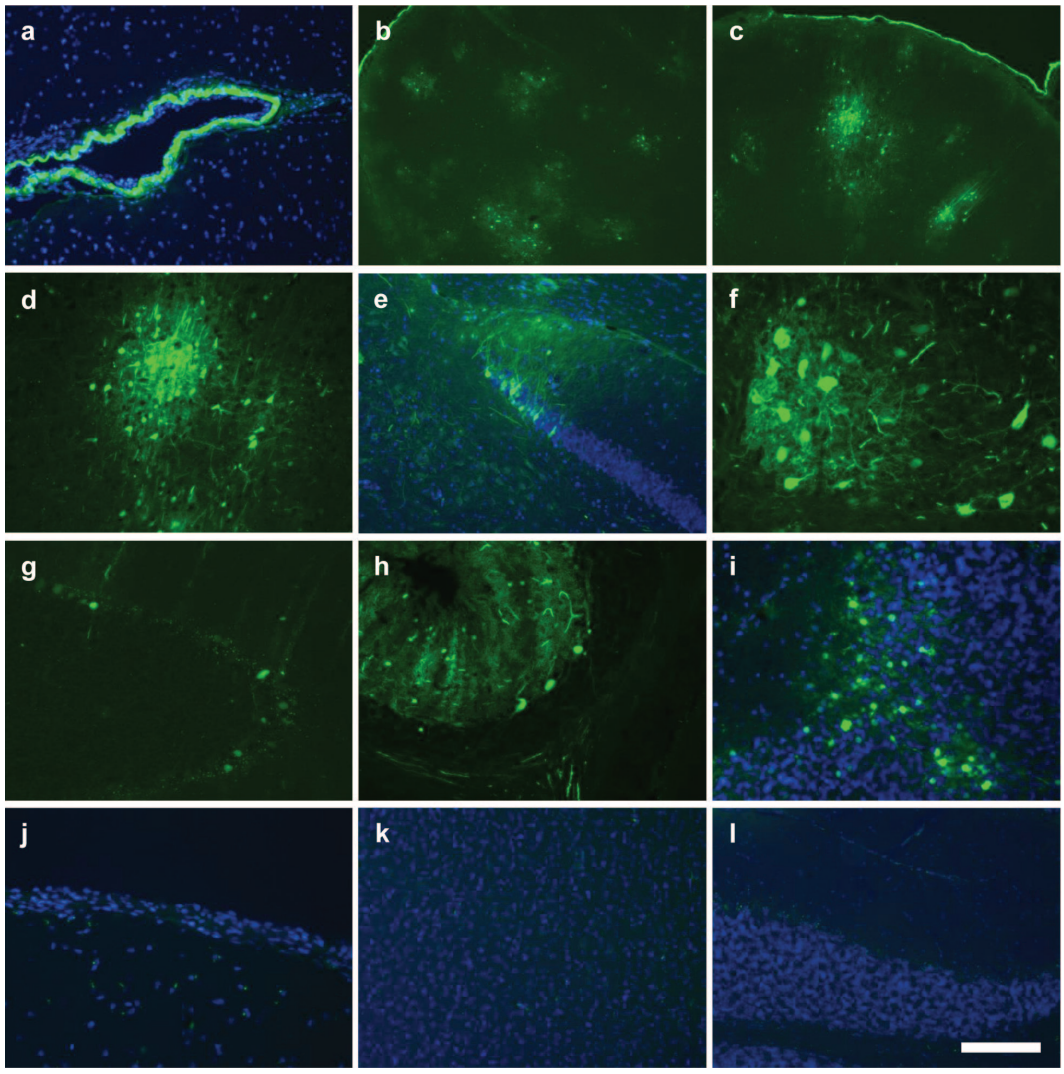

Figure 2 Transduction throughout the brain following intracisternal AAV9 delivery. AAV9 was administered to six cynomolgus macaques at doses of $2.5–5 \times 10^{12}$ GC/kg by injection into the cisterna magna ($n = 4$) or the lumbar subarachnoid space ($n = 2$). Brain sections from animals (**a**–**i**) treated by intracisternal injection and those (**j**–**l**) treated by lumbar puncture were imaged for native GFP fluorescence. (**a**,**e**,**i**–**l**) Counterstain is DAPI. All images shown were negative for fluorescence in the red channel. (**a**) Meninges (**b**–**d**) Cerebral cortex (**e**) Dentate gyrus (**f**) Thalamus (**g**,**h**) Cerebellum with large Purkinje cells. (i) Cerebellum with transduced neurons in granular layer. (**j**–**l**) Direct GFP fluorescence in (**j**) meninges, (**k**) cerebral cortex, and (**l**) cerebellum after treatment by lumbar puncture. Scale bar: (**f**,**i**,**j**) 100 µm, (**a**,**d**,**e**,**g**,**h**,**k**,**l**) 200 µm, and (**b**,**c**) 500 µm.

long been described in brain tissue, particularly when prepared by immersion fixation.[14] The high affinity of these cells for H&E did not explain their dark color in IHC sections, as the cells still appeared to stain positive when the hematoxylin counterstain was omitted from IHC sections (Supplementary Figure S1e,g). Omission of the primary antibody and both primary and secondary antibodies in combination demonstrated that the false-positive neurons did not exhibit endogenous peroxidase activity, but instead nonspecifically bound antibodies used for IHC (Supplementary Figure S1f,h). Because these false positive neurons were detected sporadically in various negative control tissues, we determined that IHC could not be used to reliably detect GFP expression in brain samples.

In order to overcome the problem of GFP false positive cells, we instead used direct GFP fluorescence to measure expression. We initially avoided this method because many cells in the CNS exhibit auto-fluorescence. We found that we could account for these fluorescence false positives by overlaying images captured in a red fluorescence channel, as GFP is detectable only in the green channel whereas auto-fluorescent material appears across several channels (Supplementary Figure S2). We therefore used direct GFP fluorescence verified by overlay with a red channel image to identify GFP positive cells. Using this method, GFP expressing cells were detected in treated animals but not in any control tissues. All subsequent analyses were carried out using this approach, and red channel images are shown for all cases in which auto-fluorescence was observed.

Intracisternal AAV9 transduces cells throughout the brain and spinal cord

Consistent with the high vector distribution to the brain in animals treated by intracisternal injection, GFP expression was observed in clusters of cells throughout most regions of the brain, which were interspersed with untransduced regions (Figure 2). Costaining with a fluorescent Nissl stain (NeuroTrace) and antibodies against astrocyte and microglial markers (GFAP and Iba1) revealed that virtually all GFP positive cells were neurons (Figure 3) although rare transduced astrocytes were also

© 2014 The American Society of Gene & Cell Therapy

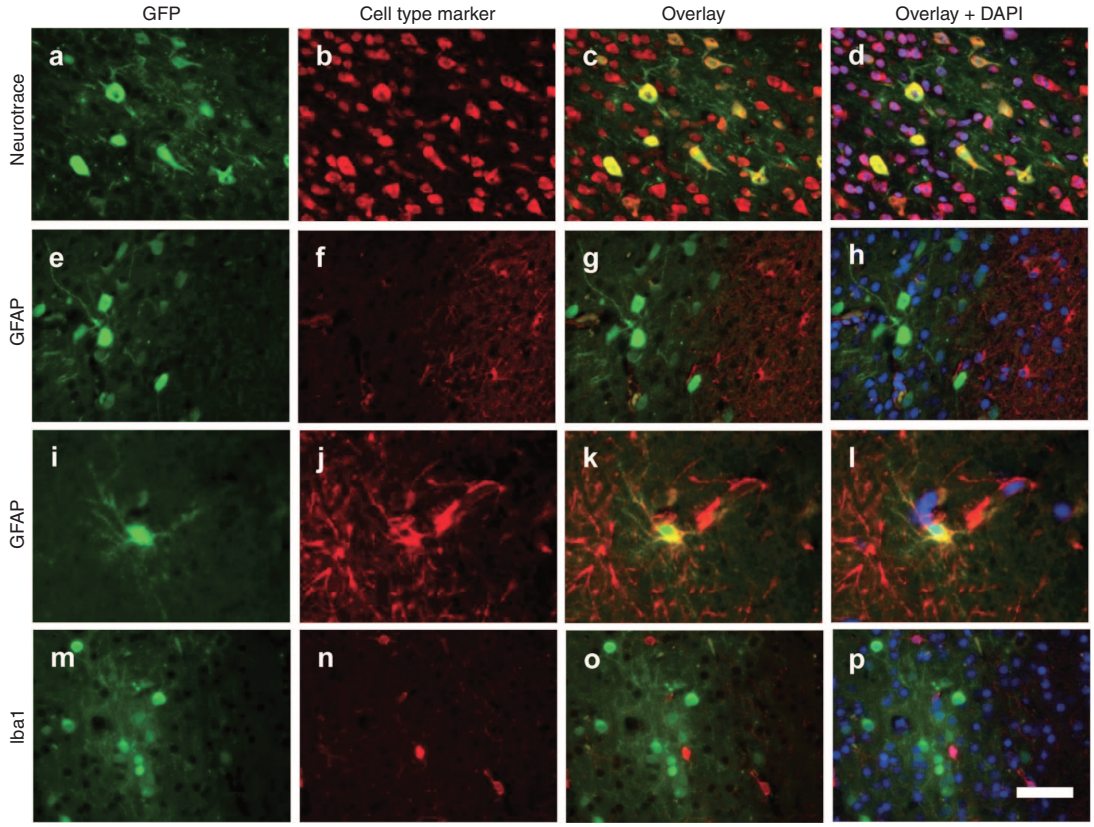

Figure 3 Predominantly neuronal transduction of intrathecal AAV9. (**a**,**e**,**i**,**m**) Cortical brain sections from animals treated by intracisternal injection were imaged for native GFP fluorescence. Images are overlaid with a (**b**–**d**) fluorescent Nissl stain (NeuroTrace) for detection of neurons, (**f**–**h**,**j**–**l**) GFAP immunostaining for astrocytes, or (**n**–**p**) Iba1 staining for microglia. (**d**,**h**,**l**,**p**) Counterstain is DAPI. Scale bar = 50 µm.

detected (Figures 3, i-1). Virtually no GFP positive cells were detected in the cerebrum of animals treated by lumbar puncture. In the spinal cord, GFP expression was prominent in the ventral horns of animals treated by intracisternal injection (Figure 4a). High magnification images show that these transduced cells were primarily the large lower motor neurons (Figure 4b). These cells were heavily transduced in the thoracic and lumbar segments of animals treated by intracisternal injection (Figure 4, Table 2). There were also a small number of transduced motor neurons in the cervical spinal cord of these animals. Transduced spinal cord cells were rare in the animals treated by lumbar administration (Table 2). The macaque treated with a high dose of intravenous AAV9 exhibited no GFP expression in the cerebrum or cerebellum, although several transduced neurons were observed in the thoracic and lumbar spinal cord (Figure 5, Table 2).

Intrathecal AAV9 does not induce an inflammatory response in the nonhuman primate brain

As one previous study reported evidence of inflammation in the cerebrum of nonhuman primates following intrathecal delivery of an AAV9 vector expressing GFP, we analyzed the brains of all treated animals for signs of inflammation.[13] No untreated animal tissues were available for histology controls, so we analyzed brains from two cynomolgus macaques that were treated with an intravenous injection of an AAV serotype 2 vector expressing erythropoietin from a liver specific promoter; these animals were previously found to have virtually no vector deposition in the brain.[15] Histopathology showed no evidence of cellular infiltrates in the brain parenchyma or in the meninges or perivascular spaces in any of the treated animals (Supplementary Figure S3). We quantified cells expressing GFAP, an intermediate filament protein that is upregulated in astrocytes in the setting of inflammation. There were no differences in the frequency of GFAP positive cells in the brains of treated animals and controls (Supplementary Figure S3 and Table S1). We also quantified microglia by Iba1 staining. The frequency of microglia was normal in all animals, and microglia exhibited morphology characteristic of a resting rather than an activated state (Supplementary Figure S3 and Table S1). Although there was no evidence of inflammation in brain tissue, we did observe a moderate lymphocytic pleocytosis in the CSF of two of the animals that were treated with intracisternal injection, which correlates with the higher CNS transduction in these animals (Supplementary Table S2).

DISCUSSION

As the first gene transfer strategy capable of achieving high levels of transduction throughout the CNS in large animals, intrathecal AAV delivery could greatly expand the applications of gene therapy in neurological disease. Intrathecal AAV injection is a particularly attractive strategy because of the relative ease of accessing the intrathecal space compared to the invasive neurosurgical procedure required for intraparenchymal injection. We found that vector delivery into the CSF at the level of the cisterna magna is far more efficient than lumbar intrathecal injection for gene transfer to the brain and spinal cord. It is interesting that the level of CSF access had such a profound effect on vector distribution, as previous work has shown that a protein infused into the lumbar CSF is distributed throughout the CNS.[16] This may therefore represent a property of the viral particle, and not reflect the behavior of other substances

© 2014 The American Society of Gene & Cell Therapy

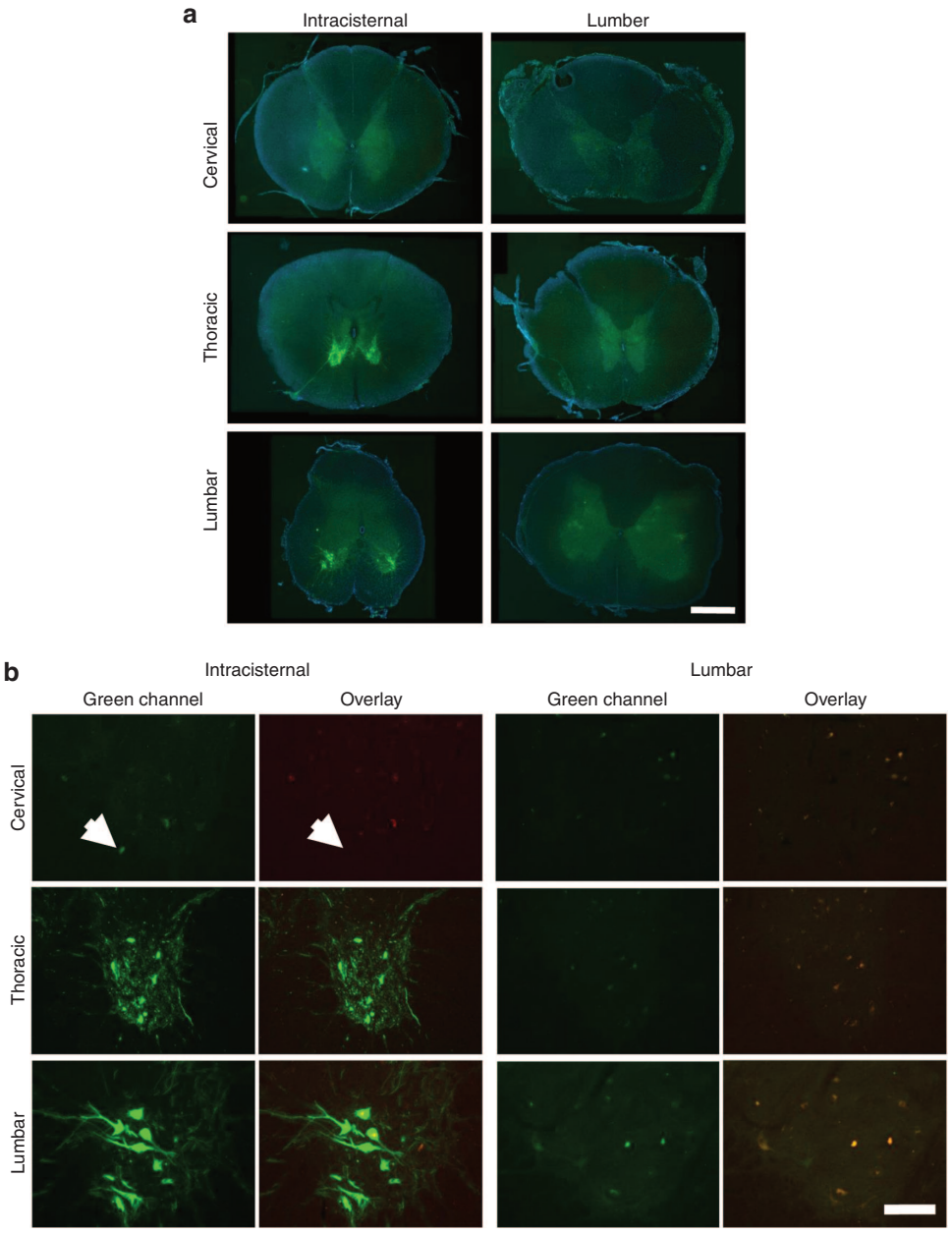

Figure 4 Spinal cord transduction following intrathecal AAV9 administration by intracisternal or lumbar injection. Direct fluorescence images were captured for three spinal cord segments from all treated animals. (**a**) Low magnification images show transduction primarily in the ventral gray matter. High magnification images of the ventral horn demonstrate transduction primarily of large neurons in the thoracic and lumbar segments, with occasional transduced cells in the cervical segment (white arrow). Scale bar: 1 mm. (**b**) As autofluorescence was observed in some spinal cord sections, an overlay of the red and green channels is shown to identify false positive GFP signal (yellow). Scale bar: 200 µm.

delivered into the intrathecal space. One potential explanation is that the vector quickly binds to cell surfaces, which would allow for wide distribution from the rapidly dispersing cisternal CSF, but not from the slower moving CSF lying inferior to the spinal cord in the lumbar cistern. Vector distribution in the CSF could be influenced by additional factors—such as the volume and formulation of the injection—which should be evaluated in future studies. Translation of this approach to humans may also benefit from further investigation of the impact of total CSF volume and cisternal volume on vector distribution, as these factors vary between species and among humans.[17]

Given the superior transduction efficiency achieved by vector delivery into the cisterna magna, it will be critical to develop a safe means of performing this procedure in patients. Though cisternal injection is commonly performed in nonhuman primates and other animals, it is infrequently utilized in clinical practice. Suboccipital puncture of the cisterna magna was first described in humans in 1920 as a technique for introduction of air or contrast material for diagnostic studies.[18] Traditional indications for cisternal puncture have also included CSF sampling. The suboccipital puncture has largely been supplanted by noninvasive diagnostic studies including CT and MRI and by CSF sampling from lower levels of the spinal canal, such as between the first and second cervical vertebrae or between lumbar vertebrae below the level of the spinal cord, techniques which are associated with lower rates of complications. The most serious complications associated with cisternal puncture

© 2014 The American Society of Gene & Cell Therapy

include inadvertent injury to vascular structures with resultant hemorrhage as well as brainstem injury. A 1929 review of the literature identified 6 reported deaths in 2019 reported procedures in 535 patients.[18] These authors also identified 9 additional cases of medullary injury, noting however that in skilled hands the procedure should not be considered dangerous.[19] In 1973, Keane again reviewed the literature finding that subarachnoid hemorrhage was the most common major complication of cisternal puncture, with at least 30 reported fatalities.[20] He noted that other serious complications resulted from direct puncture of brain substance. In 1989, Ward *et al*. evaluated cisternal puncture in cadavers, finding that "tenting" of the dura at the site of needle penetration could result in deeper than expected penetration prior to entry into the subarachnoid space.[21]

The few more recent publications available on suboccipital puncture suggest that modern day imaging equipment may improve safety by enhancing visualization of critical structures during the procedure. A recent report described better visualization of critical structures during a cisternal puncture by performing a contrast enhanced CT immediately prior to needle insertion.[22] Axial and sagittal contrast enhanced CT images (Figure 6) would allow for visualization of the entire needle path, which courses in the midline between the base of the occiput and the first vertebra to the cisterna magna. Contrast enhanced CT allows for visualization of the local vascular structures, particularly the posterior inferior cerebellar artery (PICA), which has historically been the source of bleeding in reported cases of subarachnoid hemorrhage following suboccipital puncture. Employing imaging with suboccipital puncture could also be useful for preventing damage to the medulla, a previously reported complication resulting from advancing the needle beyond the cisterna magna. The use of more sophisticated integrated navigation systems, like the Philips PercuNav system, may also provide an additional layer of safety by allowing real time needle visualization during the procedure. We therefore believe that suboccipital puncture, though uncommonly utilized, could represent a safe and feasible vector delivery approach for clinical use.

Table 2 Quantification of transduced motor neurons throughout the spinal cord

			Percent GFP⁺ motor neurons[a]		
Animal #	*ROA*	*Promoter*	*Cervical*	*Thoracic*	*Lumbar*
17	CM	CMV	ND	10.7 ± 11.4	14.5 ± 17.6
18	CM	CB	0 ± 0	8.4 ± 2.3	20.3 ± 4.9
20	CM	CB	0.3 ± 0.6	25.1 ± 17.0	19.3 ± 11.0
21	CM	CB	1.5 ± 2.1	48.0 ± 15.6	38.2 ± 23.4
04	L	CB	0.3 ± 0.6	0 ± 0	0.6 ± 1.3
05	L	CB	0 ± 0	1.7 ± 2.9	2.6 ± 5.2
49	IV	CMV	0 ± 0	7.7 ± 10.5	0.2 ± 0.5

CM, cisterna magna; IV, intravenous; L, lumbar injection; ROA, route of administration.
[a]Mean ± SD in four fields.

Consistent with previous studies, we observed efficient transduction of motor neurons in the thoracic and lumbar spinal cord following intrathecal AAV9 delivery. We found that transduction in the cerebrum, however, was much more diffuse, consisting of patches of GFP expressing cells. The transduction efficiency we observed in the brain was much lower than that reported by others, particularly following lumbar intrathecal delivery.[12] Given the potential for immunohistochemistry to produce GFP false positive cells in the CNS, it is likely that this artifact may have contributed to exaggerated transduction efficiencies in some reports. This possibility is supported by quantitative PCR data, which in one previous study show approximately one vector genome present per 100 cells in the brain—similar to our results for lumbar delivery—which would preclude transduction of the nearly 50 percent of cells identified as GFP positive by immunohistochemistry in that study.[12] Other studies of intrathecal AAV9 injection have demonstrated a pattern of brain transduction more similar to that described here.[10,11]

Clinical trials of intraparenchymal injection of AAV serotypes 2 and rh.10 have demonstrated excellent tolerability despite the

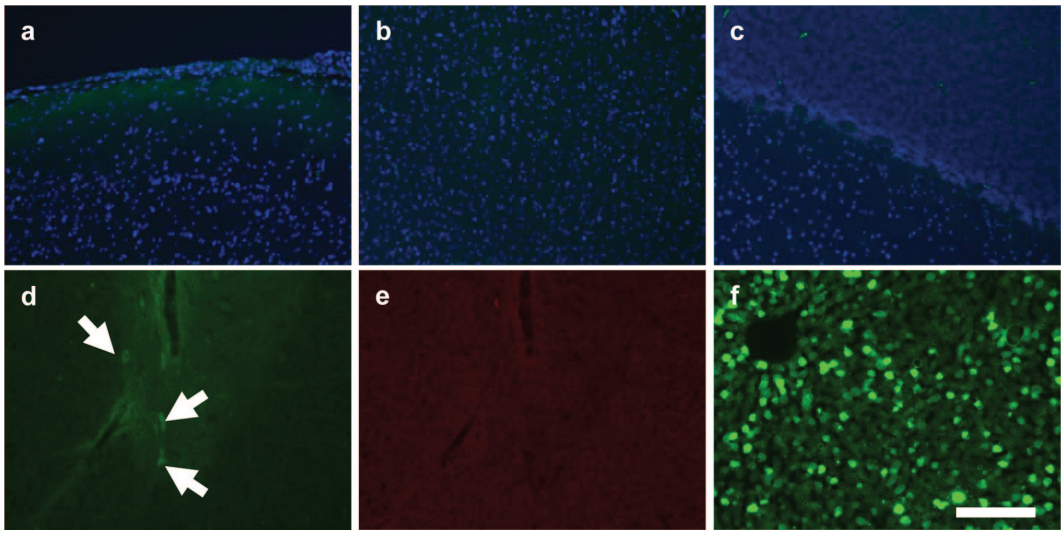

Figure 5 Limited CNS transduction following intravascular AAV9 delivery. A rhesus macaque was treated intravenously with an AAV9 vector (2×10^{13} GC/kg) expressing GFP. Sections were imaged for native GFP fluorescence from (**a**) cerebral meninges, (**b**) cortex, and (**c**) cerebellum. (**d**) Some GFP expressing cells (arrows) were noted in the thoracic spinal cord. (**e**) GFP expression was confirmed by absence of fluorescence in the red channel. (**f**) In contrast to the CNS, peripheral organs including liver were heavily transduced. Counterstain is DAPI (**a**–**c**). Scale bar: 200 µm.

© 2014 The American Society of Gene & Cell Therapy

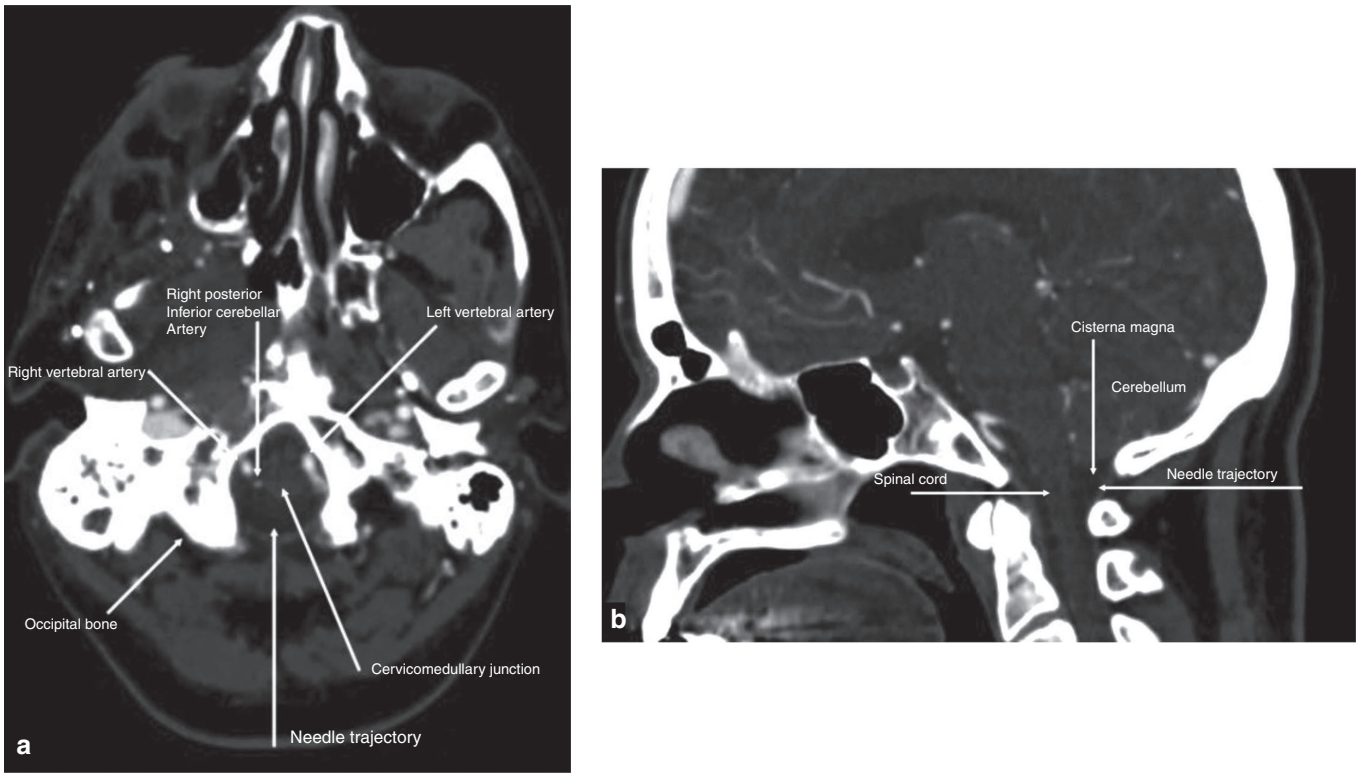

Figure 6 Evaluation of anatomic landmarks for suboccipital puncture. (**a**) Axial and (**b**) sagittal contrast enhanced CT images illustrating key structures to identify when performing a suboccipital puncture.

inherent invasiveness of this delivery method.[3–5] Several studies of intrathecal AAV9 administration in nonhuman primates have indicated that it is similarly well tolerated. However, one study reported that macaques treated with intrathecal AAV9 expressing GFP developed neurologic deficits 2–3 weeks following vector administration.[13] These animals also exhibited histological signs of inflammation in the brain, including MHC class II upregulation and microglial activation. This was presumed to be due to an immune response against the foreign GFP transgene. We did not identify similar clinical or histological findings in any treated animals. It is possible that we did not observe the same phenomenon due to our shorter follow up period (2 versus 3 weeks). However, the same group previously reported treating four macaques with intrathecal AAV9, as well as two with AAV7, both expressing GFP, without any complications during the same 3 weeks follow up period.[10,11] Likewise, another group reported no adverse events or histological abnormalities after 4 weeks of follow up in 10 macaques treated with intrathecal AAV9 expressing GFP.[12] It therefore appears that this isolated observation of an inflammatory response following intrathecal AAV9 delivery was unlikely due to the vector itself, though future studies should continue to monitor subjects for such a response. Although we did not observe any clinical or histological abnormalities, we did observe elevated CSF lymphocytes in two of the treated animals. This suggests that there may be some degree of immune activation by the vector or GFP transgene, although we have not observed any clinical or histological consequences of this response.

Our results demonstrate that delivery of an AAV9 vector into the cisterna magna is an effective approach to achieve transduction of cells throughout the nonhuman primate CNS. The excellent safety and feasibility of this route of administration should enable rapid deployment into the clinic for a wide range of diseases affecting the CNS.

MATERIALS AND METHODS

Animals

All study protocols were approved by the institutional animal care and use committee of the University of Pennsylvania. Six adult female cynomolgus macaques were used in this study. These animals were not pre-screened for AAV9 neutralizing antibodies. An additional female rhesus macaque was used for the intravenous delivery experiment. This animal was prescreened for AAV9 neutralizing antibodies as previously described.[23]

Lumbar vector injection

Animals were anesthetized using IM ketamine/dexmedetomidine. The hair over the lumbar spine was shaved and the skin sterilely prepped. To widen the intervertebral space the spine is flexed slightly, drawing the animal's hind limbs forward toward the umbilicus. A spinal needle was inserted into the center of the L3-L4 intervertebral space just behind the anterior vertebral spinous process. Needle placement was confirmed by CSF return. CSF (1 ml) was collected, then a syringe containing vector (1 ml diluted in PBS) was attached to the spinal needle through a flexible linker. Vector was slowly injected by hand over 1 minute. After injection placement was again confirmed by CSF return. The needle was removed and direct pressure applied to the puncture site.

Intracisternal vector injection

Animals were anesthetized using IM ketamine/dexmedetomidine. The hair over the back of the head and neck was shaved and the skin sterilely prepped. The occipital protuberance at the back of the skull and the wings of the atlas (C1) were palpated, and a needle was inserted midway between them. Needle placement was confirmed by CSF return. CSF (1 ml) was collected, then a syringe containing vector (1 ml diluted in PBS) was attached to the needle through a flexible linker. Vector was slowly injected by hand over one minute. After injection placement was again confirmed by CSF return. The needle was removed and direct pressure applied to the puncture site.

Vector production

Single-stranded AAV9 vectors were produced by triple transfection of 293 cells and purified by iodixanol gradient centrifugation as previously described.[23]

© 2014 The American Society of Gene & Cell Therapy

Quantitative PCR

Vector genomes were quantified in tissue samples by Taqman PCR as previously described.[23]

Histology

Brains were divided into left and right hemisphere. The right half was sliced, fixed in formalin overnight, and embedded in paraffin for the preparation of H&E stained sections and for immunostaining. Slices from the left half were formalin-fixed and processed for GFP detection as described below. PCR samples for vector biodistribution studies were also retrieved from the left brain half prior to fixation. Tissues from spinal cord was collected from cervical, thoracic, and lumbar regions and processed for paraffin and cryosections as described for the brain.

Hematoxylin and eosin staining (H&E)

H&E staining was performed on 6 µm paraffin sections according to standard protocols.

GFP fluorescence

Brain slices were fixed overnight in formalin, equilibrated sequentially in 15 and 30% sucrose in PBS, and frozen in OCT embedding medium for the preparation of cryosections for visualization of direct GFP fluorescence. Sections were mounted in Vectashield containing DAPI (Vector Laboratories, Burlingame, CA) as nuclear counterstain.

Immunohistochemistry for GFP

Sections were deparaffinized through an ethanol and xylene series, boiled in a microwave for 6 minute in 10 mmol/l citrate buffer (pH 6.0) for antigen retrieval, treated sequentially with 2% H_2O_2 (15 minute), avidin/biotin blocking reagents (15 minute each; Vector Laboratories), and blocking buffer (1% donkey serum in PBS + 0.2% Triton for 10 min) followed by incubation with primary (1 hour) and biotinylated secondary antibodies (45 minute; Jackson Immunoresearch, West Grove, PA) diluted in blocking buffer. As primary antibodies served a rabbit serum or a chicken antibody against GFP (both from Abcam, Cambridge, MA; diluted 1:1,000) which both yielded similar results. A Vectastain Elite ABC kit (Vector Laboratories) was used according to the manufacturer's instructions with DAB as substrate to visualize bound antibodies as brown precipitate. Sections were slightly counterstained with hematoxylin to show nuclei. In some experiments, hematoxylin counterstaining or antibodies were omitted as described in the text.

Immunofluorescence

Immunostaining was performed on sections from formalin-fixed paraffin-embedded tissue samples. Sections were deparaffinized and treated for antigen retrieval as described above, then blocked with 1% donkey serum in PBS + 0.2% Triton for 15 minutes followed by sequential incubation with primary (1 hour) and fluorescence-labeled secondary antibodies (45 minutes) diluted in blocking buffer. Primary antibodies used were goat antibodies against GFAP (Novus Biologicals, Littleton, CO; 5 µg/ml working concentration) and Iba1 (Abcam, 1:200), and TRITC-labeled donkey anti-goat (Jackson Immunoresearch, 1:100) served as secondary antibody.

Morphometric analyses

To quantify astrocytes (GFAP-positive cells) and microglia (Iba1-positive cells), 15 images were taken from immunostained brain sections per animal with a 20× objective showing the area directly below the cerebral cortex surface. Positive cells were counted manually and averaged for each animal. Brain tissues from two cynomolgus macaques from an unrelated study that had received AAV2.TGB.EPO intravenously and showed negligible vector genome copy numbers in the brain (below 1×10^{-4} gc/cell) served as controls.[15]

For the quantification of transduced motor neurons, spinal cord sections were stained with Neurotrace red fluorescent Nissl stain (Life Technologies, Grand Island, NY) according to the manufacturer's instructions and images were taken at low magnification (4× objective) showing GFP expression and Neurotrace staining. Between three to five images were taken from the ventral area of each spinal cord region (cervical, thoracic, lumbar) to cover several sections per animal. ImageJ software (Rasband W. S., National Institutes of Health, USA; http://rsb.info.nih.gov/ij/) was used to first threshold and then select all Neurotrace-positive cells with a minimum pixel number of 175 reflecting a threshold diameter of ~25 µm. To determine the percentage of size-selected neurons that were GFP-positive, all selected neurons and those that were GFP-positive were counted for each image.

ACKNOWLEDGMENTS

We thank Yanqing Zhu (Gene Therapy Program, University of Pennsylvania Perelman School of Medicine) for expert histology services and Jenny Greig (Gene Therapy Program, University of Pennsylvania Perelman School of Medicine) for assistance with figure preparation. We acknowledge the support of the vector, immunology, and animal models cores of the Gene Therapy Program. This work was funded by a grant from ReGenX Holdings (J.M.W.).

CONFLICT OF INTEREST

J.M.W. is an advisor to ReGenX Biosciences and Dimension Therapeutics, and is a founder of, holds equity in, and receives grants from ReGenX Biosciences and Dimension Therapeutics; in addition, he is a consultant to several biopharmaceutical companies and is an inventor on patents licensed to various biopharmaceutical companies.

REFERENCES

1. Haurigot, V, Marco, S, Ribera, A, Garcia, M, Ruzo, A, Villacampa, P, *et al*. (2013). Whole body correction of mucopolysaccharidosis IIIA by intracerebrospinal fluid gene therapy. *J Clin Invest* **123**: 3254–3271.
2. Wolf, DA, Lenander, AW, Nan, Z, Belur, LR, Whitley, CB, Gupta, P *et al*. (2011). Direct gene transfer to the CNS prevents emergence of neurologic disease in a murine model of mucopolysaccharidosis type I. *Neurobiol Dis* **43**: 123–133.
3. Tardieu, M, Zerah, M, Husson, B, de Bournonville, S, Deiva, K, Adamsbaum, C *et al*. (2013). Intra cerebral administration of AAVrh.10 carrying human SGSH and SUMF1 cDNAs in children with MPSIIIA disease: result of a phase I/II trial. *Hum Gene Ther* **24**: A23–A24.
4. Kaplitt, MG, Feigin, A, Tang, C, Fitzsimons, HL, Mattis, P, Lawlor, PA *et al*. (2007). Safety and tolerability of gene therapy with an adeno-associated virus (AAV) borne GAD gene for Parkinson's disease: an open label, phase I trial. *Lancet* **369**: 2097–2105.
5. McPhee, SW, Janson, CG, Li, C, Samulski, RJ, Camp, AS, Francis, J *et al*. (2006). Immune responses to AAV in a phase I study for Canavan disease. *J Gene Med* **8**: 577–588.
6. Vite, CH, McGowan, JC, Niogi, SN, Passini, MA, Drobatz, KJ, Haskins, ME *et al*. (2005). Effective gene therapy for an inherited CNS disease in a large animal model. *Ann Neurol* **57**: 355–364.
7. McCurdy, VJ, Johnson, AK, Gray-Edwards, HL, Randle, AN, Brunson, BL, Morrison, NE *et al*. (2014). Sustained normalization of neurological disease after intracranial gene therapy in a feline model. *Sci Transl Med* **6**: 231ra48.
8. Bevan, AK, Duque, S, Foust, KD, Morales, PR, Braun, L, Schmelzer, L *et al*. (2011). Systemic gene delivery in large species for targeting spinal cord, brain, and peripheral tissues for pediatric disorders. *Mol Ther* **19**: 1971–1980.
9. Gray, SJ, Matagne, V, Bachaboina, L, Yadav, S, Ojeda, SR and Samulski, RJ (2011). Preclinical differences of intravascular AAV9 delivery to neurons and glia: a comparative study of adult mice and nonhuman primates. *Mol Ther* **19**: 1058–1069.
10. Samaranch, L, Salegio, EA, San Sebastian, W, Kells, AP, Foust, KD, Bringas, JR *et al*. (2012). Adeno-associated virus serotype 9 transduction in the central nervous system of nonhuman primates. *Hum Gene Ther* **23**: 382–389.
11. Samaranch, L, Salegio, EA, San Sebastian, W, Kells, AP, Bringas, JR, Forsayeth, J *et al*. (2013). Strong cortical and spinal cord transduction after AAV7 and AAV9 delivery into the cerebrospinal fluid of nonhuman primates. *Hum Gene Ther* **24**: 526–532.
12. Gray, SJ, Nagabhushan Kalburgi, S, McCown, TJ and Jude Samulski, R (2013). Global CNS gene delivery and evasion of anti-AAV-neutralizing antibodies by intrathecal AAV administration in non-human primates. *Gene Ther* **20**: 450–459.
13. Samaranch, L, San Sebastian, W, Kells, AP, Salegio, EA, Heller, G, Bringas, JR *et al*. (2014). AAV9-mediated expression of a non-self protein in nonhuman primate central nervous system triggers widespread neuroinflammation driven by antigen-presenting cell transduction. *Mol Ther* **22**: 329–337.
14. Jortner, BS (2006). The return of the dark neuron. A histological artifact complicating contemporary neurotoxicologic evaluation. *Neurotoxicology* **27**: 628–634.
15. Gao, G, Lu, Y, Calcedo, R, Grant, RL, Bell, P, Wang, L *et al*. (2006). Biology of AAV serotype vectors in liver-directed gene transfer to nonhuman primates. *Mol Ther* **13**: 77–87.
16. Calias, P, Papisov, M, Pan, J, Savioli, N, Belov, V, Huang, Y *et al*. (2012). CNS penetration of intrathecal-lumbar idursulfase in the monkey, dog and mouse: implications for neurological outcomes of lysosomal storage disorder. *PLoS ONE* **7**: e30341.

© 2014 The American Society of Gene & Cell Therapy

17. Whitney, N, Sun, H, Pollock, JM and Ross, DA (2013). The human foramen magnum–normal anatomy of the cisterna magna in adults. *Neuroradiology* **55**: 1333–1339.
18. Ayer, JB (1920). Puncture of the cisterna magna. *Arch Neurol Psychiatry* **4**: 529–541.
19. Saunders, HC and Riordan, TJ (1929). Cisternal or suboccipital puncture. *N Engl J Med* **201**: 166–168.
20. Keane, JR (1973). Cisternal puncture complications. Treatment of coccidioidal meningitis with amphotericin B. *Calif Med* **119**: 10–15.
21. Ward, E, Orrison, WW and Watridge, CB (1989). Anatomic evaluation of cisternal puncture. *Neurosurgery* **25**: 412–415.
22. Pomerantz, S, Buchbinder, B and Hirsch, J (2005). Suboccipital puncture of the cisterna magna under CT-guidance with intravenous enhancement in order to circumvent anomalous course of posterior inferior cerebellar artery. American Society of Spine Radiology (meeting abstract). http://theassr.org/abstract/suboccipital-puncture-of-the-cisterna-magna-under-ct-guidance-with-intravenous-enhancement-in-order-to-circumvent-anomalous-course-of-posterior-inferior-cerebellar-artery-pica/
23. Wang, L, Calcedo, R, Bell, P, Lin, J, Grant, RL, Siegel, DL *et al*. (2011). Impact of pre-existing immunity on gene transfer to nonhuman primate liver with adeno-associated virus 8 vectors. *Hum Gene Ther* **22**: 1389–1401.

This work is licensed under a Creative Commons Attribution-NonCommercial-NoDerivs 3.0 Unported License. The images or other third party material in this article are included in the article's Creative Commons license, unless indicated otherwise in the credit line; if the material is not included under the Creative Commons license, users will need to obtain permission from the license holder to reproduce the material. To view a copy of this license, visit http://creativecommons.org/licenses/by-nc-nd/3.0/

Supplementary Information accompanies this paper on the *Molecular Therapy—Methods & Clinical Development* website (http://www.nature.com/mtm)